Simultaneous T1, T2, PD, and B1 mapping with dual angle IR-bSSFP (DAIRy-bSSFP)

R. D. Newbould[1], M. T. Alley[1], G. Gold[1], and R. Bammer[1]
[1]Radiology, Stanford University, Stanford, CA, United States

Introduction It has been shown that an IR-bSSFP sequence may be used to concurrently map T1, T2, and proton density (PD)[1-4]. However, this method is problematic in practice due to its extreme dependence upon the flip angle achieved[5]. Although 3D methods remove much of the error from RF slice profile effects, the applied transmit RF (B_1^+) field is never homogenous in practice. The B_1^+ field variation markedly increases with field strength and decreasing size of the transmit coil. Here, the method is extended to additionally map the B_1^+ field to correct the parameter estimation.

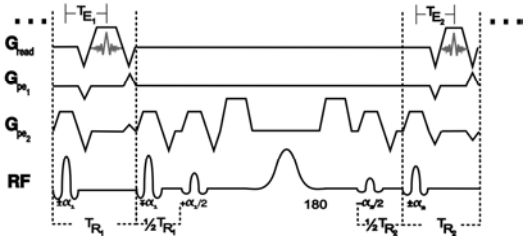

Figure 1. IR-bSSFP Sequence transition diagram. A -½ α pulse ½ TR after the last α pulse pushes the steady-state magnetization longitudinally, before adiabatic reinversion, and a bSSFP playout with a new flip angle.

The relative changes in the determined values of the T1 and PD (dubbed $\hat{T}_1$ and $\hat{PD}$) do not depend on the underlying true T1, T2, or PD, but only the change in the achieved flip angle (α) versus the assumed flip angle (ά)[5]. The achieved excitation angle over the space vector **r** is a direct function of the spatially-dependent B_1^+ field and the RF pulse form $f(t)$. If it is assumed that the RF pulses are approximately non slice-selective and <~100°, not unreasonable for a 3D bSSFP sequence, the achieved B_1^+ field can be written as[6]: $\alpha(\mathbf{r}) = \gamma \cdot B_1^+(\mathbf{r}) \cdot \int f(t)dt = B_1^+(\mathbf{r}) \cdot \dot{\alpha}$. Thus, it is possible to express the change in T1, T2, or PD as a function of the excitation field. Here, the formula for T_1 has been chosen, as it has the greatest change between chosen flip angles (though is also least sensitive to B_1^+ variation). For a set of N IR-bSSFP experiments, each with some desired flip angle $\dot{\alpha}_n$, $T_1(\mathbf{r}) = \cos(\dot{\alpha}_n) \cdot \hat{T}_1 \Big/ \cos(B_1^+(\mathbf{r}) \cdot \dot{\alpha}_n)$. As the true T_1 value does not change between experiments, a series of N equations may be solved for $B_1^+(\mathbf{r})$. This procedure would, however, require performing at least two separate IR bSSFP experiments, using different flip angles, doubling scan time.

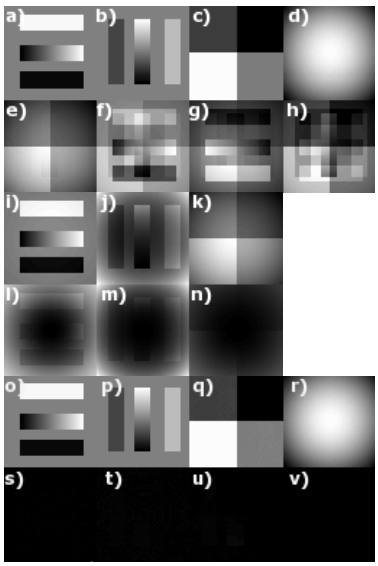

Figure 2. T1, T2, PD and B1 mapping with the dual-angle IR-bSSFP. Top row contains the a)T1, b)T2, c)M0 and d)B1 used for Bloch simulation, and e)-h) are timepoint images from the progression to steady state. IR-bSSFP mapping characterizes i)T1, j)T2, and k)PD, however, difference images [l)-n)] show errors from the B1 field, which varies down to 80% at the periphery. DAIRy-bSSFP mapping determines the B1 field [r)], which can correct the parameter maps [o)-q)]. Difference images [s)-v)] are negligible.

Instead, the IR-bSSFP sequence was modified to transition from one steady state into a second full IR curve, in order to perform a dual-angle IR-bSSFP (DAIRy-bSSFP) for concurrent T1, T2, PD, and B1 estimation. After inversion, the $\dot{\alpha}_A/2$ prep is continued by the phase-alternating $\dot{\alpha}_A$ pulses and sampled for the first measurement time, T_{MA}, while it is progressing towards $S_{STST\text{-}A}$. At the end of the measurement time, the magnetization is forced back to the longitudinal axis by a $-\dot{\alpha}_A/2$ pulse a half-TR after the last full $\dot{\alpha}_A$ pulse. Any residual transverse magnetization is crushed, and a second adiabatic inversion pulse is applied to the longitudinal magnetization, which has magnitude of $S_{STST\text{-}A}$. After the inversion, a second measurement is performed with *different* flip angle $\dot{\alpha}_B$ in the same manner as the first measurement. Finally, after the second measurement time T_{MB} has elapsed, magnetization is allowed to relax back to M_0. An analogous transition method in SSFP has been previously demonstrated for fat-saturated steady-state imaging[7]. Any difference between these values determined by the first and second trains is due to B_1^+ inhomogeneity. Thus, the B_1^+ field may be solved by equating, e.g., the T_1's determined by each separate pulse train: $T_{1_A}^* \cdot \cos(B_1(\mathbf{r}) \cdot \dot{\alpha}_A) \cdot \sin(\dot{\alpha}_A/2) \Big/ S_{stst_A} = T_{1_B}^* \cdot \cos(B_1(\mathbf{r}) \cdot \dot{\alpha}_B) \cdot \sin(\dot{\alpha}_B/2) \Big/ S_{stst_B}$.

In practice, noise in the images perturbs the calculated B_1^+ field, thus, after calculation, the B_1^+ field is fitted with a 3rd order polynomial, in order to force a smoothly varying B_1^+ field.

Materials and Methods The DAIRy-bSSFP sequence was Bloch simulated using a numerical phantom of varying T1, T2, and PD values, and a B1 field. The sequence was then implemented on a GE Signa EXCITE 3.0T platform, and images were acquired using the quadrature head coil. A uniform cylindrical Gd-DTPA doped agar phantom with a T_1 of 1354 ms and T_2 of 45 ms at 3T, as determined by IR-SE and CPMG FSE sequences, was imaged using 128x128 matrix, $\dot{\alpha}_A$=50°, $\dot{\alpha}_B$=30°, 28 spiral intlvs, TR=3.35ms, T_{MA}=4s, T_{MB}=4s.

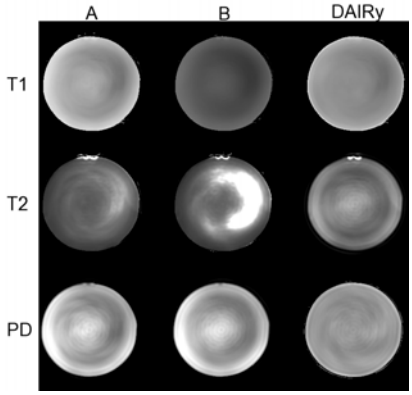

Figure 3. IR-bSSFP relaxometry is hampered by the B1 field. Columns A and B show parameters determined by each of the two trains in DAIRy-bSSFP. Their combination allows B1-mapping, which can help to correct the parameter maps.

Results Fig 2 shows the Bloch simulation results using the a)T1, b)T2, c)PD, and d)B1 field shown. The B1 field influences the veracity of the relaxometry results (3rd row), especially the T2 values, as evident in the difference images (4th row). The DAIRy sequence can use the variation in parameter calculation between the two trains to find the B1 map, which can correct the parameter results (5th row). Difference images are negligible (6th row). Phantom imaging on the 3T system are shown in Figure 3. The first and second columns show the parameters calculated from the first and second halves of the DAIRy train, each of which is an IR-bSSFP experiment. The B1 variation greatly influences the results, especially the gross overestimation of T2 in regions of low achieved flip angle. However, when taken together, the two trains allowed a B1 map to be calculated, which could be used to improve the fits.

Conclusion. Relaxometry with IR-bSSFP has promise to simultaneously map all three intrinsic tissue parameters. However, its extreme dependence on the B1 field precluded its use. Here, the method was extended such that the B1 field could be concurrently determined using a dual-angle approach. The field map could then be used to correct the quantitative parameters.

References. [1]Scheffler K. MRM 2003;49(4):781-783. [2]Scheffler K, *et al*. MRM 2001;45(4):720-723. [3]Schmitt P, *et al*. MRM 2004;51(4):661-667. [4]Gulani V, *et al*. Invest Radiol 2004;39(12):767-774. [5]Newbould R, *et al*. 13th ISMRM, 2005, p. 2191. [6]Stollberger R, et al. MRM 1996;35:246-251. [7]Scheffler K, et al. MRM 2001;45:1075-1080. **Acknowledgements.** This work was supported in part by the NIH (1R01EB002711), the Center of Advanced MR Technology at Stanford (P41RR09784), Lucas Foundation, and Oak Foundation.